ELSEVIER

Journal of Nuclear Materials 290–293 (2001) 61–65

journal of nuclear materials

www.elsevier.nl/locate/jnucmat

Methane formation in graphite and boron-doped graphite under simultaneous O^+ and H^+ irradiation

A.Y.K. Chen *, J.W. Davis, A.A. Haasz

Fusion Research Group, University of Toronto, Institute for Aerospace Studies, 4925 Dufferin St., Toronto, Ont., Canada M3H 5T6

Abstract

Boron-doped graphite specimens (~15 at.% B) exposed to simultaneous O^+/H^+ irradiation were found to have higher methane yields than when exposed to H^+ ions alone. This finding is opposite to the case of pure graphite where simultaneous O^+/H^+ irradiation leads to a decrease in methane yield when compared to the H^+-only case. It appears that the mechanism leading to CH_4 yield reduction for B-doped graphites is partially nullified by the presence of oxygen ions. Possible mechanisms are proposed.

Keywords: Boronized graphite; Chemical erosion; Ion bombardment; Oxygen; Boron

1. Introduction

Oxygen is often one of the main intrinsic impurities in the plasma of current fusion devices with carbon first walls. Therefore, the synergistic reactions of oxygen-containing ions and the hydrogenic fuel with carbon materials play an important role in the complex process of plasma wall interaction. Carbon erosion due to separate bombardment by H^+ and O^+ has been studied extensively, but only limited data exist currently on the effect of exposing carbon-based materials simultaneously to energetic oxygen and hydrogen [1–4]. Our previous investigation of the temperature dependence of chemical erosion yields has demonstrated the formation of water molecules during simultaneous H^+ and O^+ bombardment of graphite [3]. In addition, small reductions for both the CO and CO_2 yields during H^+–$O^+ \rightarrow$ C reactions as compared to $O^+ \rightarrow$ C cases, and reductions in CH_4 yields during H^+–$O^+ \rightarrow$ C reactions as compared to $H^+ \rightarrow$ C, were observed [3]. Further details of the mechanisms of the interaction between the oxygen ions and hydrogen ions in the carbon system were revealed by varying the energy (i.e., the implantation depth) and the flux ratio (Φ_O/Φ_H) of the two ion beams [4].

It was found that ion range has a negligible effect on the H_2O yield, as well as on the reduction of CO, CO_2 and CH_4 formations during O^+–$H^+ \rightarrow$ C reactions, as compared to $O^+ \rightarrow$ C or $H^+ \rightarrow$ C reactions [4]. The independence of H_2O yield (and the resulting CO and CO_2 yield reduction) on the energy separation was thought to be caused by the ability of hydrogen to freely travel on internal surfaces in the modified implantation zone to react with the immobile trapped oxygen [4]. Methane reduction was explained by a separate phenomenon: methane molecule break-up due to energetic oxygen bombardment as they make their way out of graphite [4–6]. The relative changes of CO, CO_2, and CH_4 yields, as well as H_2O production, however, do depend on the Φ_O/Φ_H flux ratio. The reductions of CO/O^+ and CO_2/O^+ yields during H^+ and O^+ co-bombardment are the highest for 'small' flux ratios (Φ_O/Φ_H); the corresponding water yield (H_2O/O^+) is also the highest for 'small' flux ratios [4]. This was explained by the relative abundance of hydrogen concentration for the formation of water in the small flux ratio cases [4]. On the other hand, the reductions of CH_4/H^+ yields during H^+ and O^+ co-bombardment, as compared to $H^+ \rightarrow$ C reactions, are the highest for 'large' Φ_O/Φ_H flux ratios. This was explained by the high concentration

* Corresponding author. Tel.: +1-416 667 7891; fax: +1-416 667 7799.

E-mail address: allen@starfire.utias.utoronto.ca (A.Y.K. Chen).

0022-3115/01/$ - see front matter
PII: S0022-3115(00)00620-6

of energetic oxygen ions breaking up more methane molecules.

Doped graphite provides an interesting opportunity to further examine the mechanisms of the synergistic effect in the O^+–$H^+ \rightarrow C$ interaction described above. From the previous studies with doped graphites under hydrogen ion irradiation, it was observed that hydrocarbon yields could be reduced by the presence of dopants [7]. In particular, boron-doping can lead to CH_4 yield reductions by as much as a factor of 5. Other studies have shown a similar dramatic reduction in chemical erosion yields through boron-doping of graphite; see [8–13]. The precise mechanism for this resistance to erosion is still largely unknown. It was suggested [7] that boron somehow enhances the recombination of mobile hydrogen atoms, which in turn lowers the CH_4 yields through reduction of the available hydrogen supply. Alternatively, the presence of boron impurities in the graphite crystallite may alter the chemistry of hydrocarbon precursor formation. It has been suggested [2] that, with the presence of boron dopants, irradiation with energetic hydrogen leads to an increase of the sp^3-hybridization states of the C atoms, resulting in reduced chemical erosion and a shift in the erosion maximum to lower temperatures (as is evident in [7–13]). As will become evident in the discussion below, the present results on methane formation during O^+–H^+ irradiation of B-doped graphite cannot be fully explained by this theory.

The objective of the present study is to investigate what happens during simultaneous O^+–H^+ bombardment of B-doped carbon (i.e., O^+–$H^+ \rightarrow C/B$). Boron-doped graphite may reveal further clues about mechanisms leading to synergistic effects in the O^+–$H^+ \rightarrow C$ reaction system. In turn, the O^+–$H^+ \rightarrow C/B$ reaction system may provide information leading to the understanding of the CH_4 yield reduction mechanism due to boron in the $H^+ \rightarrow C/B$ system.

2. Experimental setup

The erosion of graphite has been studied under conditions of simultaneous bombardment by O_2^+ and H_3^+ ions, using an independently controlled high-flux, low-energy, mass-analyzed dual-beam ion accelerator system [14]. The hydrogen ions are produced from a pure hydrogen gas by a duoplasmatron ion source with a hot filament cathode coated with a barium-containing compound. The oxygen ions are produced from a 10%-oxygen/90%-helium gas mixture by a modified duoplasmatron ion source fitted with a stainless steel hollow cathode. From previous studies of methane formation from graphite under energetic H^+ and H_3^+ irradiation, the H_3^+ molecular ions were found to behave effectively as three hydrogen atoms with one-third of the H_3^+ ion energy [15]. Thus, it is assumed that the incident O_2^+ and H_3^+ molecular ions break up immediately into atoms upon impact with the specimen, and act independently within the graphite. Here, we use H^+ and O^+ to designate incident particles even though not all of the atoms in the incident molecular ions are charged. The two beams impact on the specimen at 21° to the normal, with 42° beam separation.

For the present study, the beam energies were in the ranges 0.7–3 keV/H^+ and 5 keV/O^+, with the energy ratio (E_O/E_H) being in the range 1.6–7.1. The approximate depth profiles of both O^+ and H^+ beams, based on the energies used, were calculated using the TRVMC program [16] assuming a graphite target doped with 15 at.% boron with a density of ~2000 kg/m^3; see Fig. 1. The calculated profiles are similar to the pure graphite case [4]. Hydrogen beam fluxes were in the range $0.6–3.1 \times 10^{19}$ H^+/m^2 s, while the oxygen beam flux was fixed at $\sim 3 \times 10^{18}$ O^+/m^2 s. The flux ratio (Φ_O/Φ_H) was in the range ~10–50%. The beam spots, slightly elliptical in shape due to off-normal incidence, were ~5 mm (for H^+) and ~3 mm (for O^+) in diameter. This allowed complete overlapping of the O^+ beam spot by the H^+ beam on the specimen. In essence, the experimental procedures for the flux/energy dependence study of pure graphite described in [4] were followed here for B-doped specimens.

Two types of boron-doped carbon specimens were used, both were cut into $25 \times 10 \times 0.5$ mm^3 strips. The first specimen was cut from a block of doped graphite prepared by Ceramics Kingston Ceramique (CKC), manufactured from finely ground graphite (10–45 μm) mixed with an organic binder with boron added as B metal particulates of ~μm size. The specimen contains about 20 at.% B in the bulk (depth > 1 μm), and about

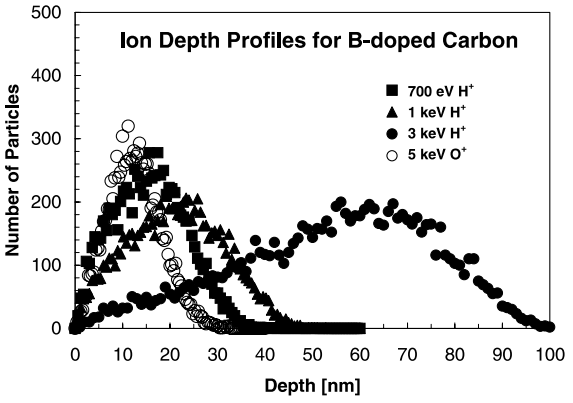

Fig. 1. Implantation depth profiles for H^+ and O^+ in graphite calculated by the TRVMC [16] program for graphite doped with 15 at.% boron, assuming a density of ~2000 kg/m^3. We note that implantation profiles in 14 and 15 at.% doped carbon are essentially the same; hence we only show the 15 at.% B case.

14 at.% B on the surface (depth < 1 μm). It has a measured density of 1970 kg/m^3. This is the same material that was designated as CKC-B20-base in the experiment described in [7]. For consistency with previous papers, we have retained the CKC-B20 designation even though the relevant B concentration for our study is the near-surface concentration of ~14 at.% B. The second specimen (USB15) was a fine-grain (~0.01 μm) boron-doped graphite manufactured by NII Grafit USSR with a density of ~2000 kg/m^3 and a uniform distribution of 15 at.% boron [11].

The target chamber in which the specimen was housed was baked for at least 24 h at ~500 K before the experiments. The specimen was annealed to >1200 K prior to the experiments. Reaction products were measured by quadrapole mass spectrometry (QMS) in both residual gas analysis (RGA) and line-of-sight (LOS) modes, after steady-state CH_4 production was attained. Although it would be interesting to study the evolution of the surface concentrations of B, O, and C, such transient measurements were not performed. A computer-controlled data acquisition system was used to collect the QMS data. The absolute erosion yield of methane was obtained by using commercially produced calibrated leaks with an absolute error of 20%.

3. Results and discussions

As with the O^+–$H^+ \rightarrow$ C interaction, no re-emission of O or O_2 was observed in the LOS detection mode for both the $O^+ \rightarrow$ C/B and O^+–$H^+ \rightarrow$ C/B irradiation of the CKC-B20 and USB15 specimens. However, some decrease of water yield (H_2O/O^+) was observed for the O^+–$H^+ \rightarrow$ C/B reactions when compared to the O^+–$H^+ \rightarrow$ C reactions; the water results will be presented elsewhere [17]. The single most obvious difference between the O^+–$H^+ \rightarrow$ C and O^+–$H^+ \rightarrow$ C/B cases is the CH_4 yield during simultaneous O^+ and H^+ impact. Fig. 2 shows the raw trace of a typical experimental run in the RGA mode (at ~800 K) for both the O^+–$H^+ \rightarrow$ C (pyrolytic graphite) [4] and O^+–$H^+ \rightarrow$ C/B (CKC-B20) experiments. We can see immediately that, compared to H^+ only irradiation, CH_4 yields are higher during simultaneous O^+ and H^+ irradiation, while for the O^+–$H^+ \rightarrow$ C case the CH_4 yields are lower during simultaneous O^+ and H^+ irradiation. Similar results were observed for O^+–$H^+ \rightarrow$ C/B irradiation of the USB15 specimen.

We note that the B_xO_y formed from the above-mentioned combination of B and O during simultaneous O^+ and H^+ irradiation of boron-containing graphite (also observed by XPS in TEXTOR [21]) may be slowly removed by energetic H^+ when the oxygen is no longer in the system, i.e., after the O^+ is turned off. This removal of B_xO_y molecules is largely due to physical sputtering below 1200 K, as observed in the studies of the $O^+ \rightarrow B_4C$ system [22,23]. The presence of B_xO_y and its removal by H^+ are likely to be the cause of the transient behaviour seen in Fig. 2(b), where the CH_4 yield decreases very slowly after the O^+ beam is turned off. Although no attempt was made here to study the production of B_xO_y species, future studies shall include the monitoring of BO to examine the relationship of its yield to the synergistic effects in the O^+–$H^+ \rightarrow$ C/B system.

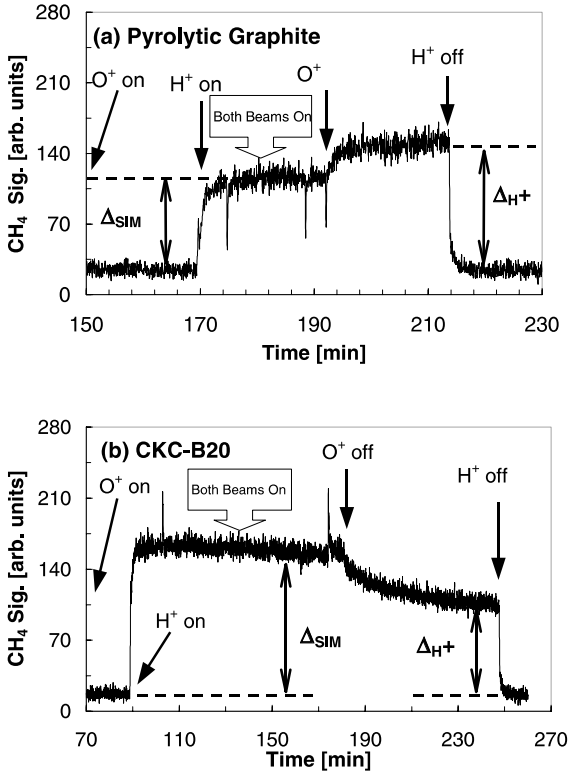

Fig. 2. CH_4 QMS (mass 15) signal trace in the RGA detection mode at 800 K for (a) O^+–$H^+ \rightarrow$ C (pyrolytic graphite) with beam ranges overlapping ($E_O = 5$ keV, $E_H = 0.7$ keV, $\Phi_O \sim 3.1 \times 10^{18}$ O^+/m^2 s, $\Phi_H \sim 1 \times 10^{19}$ H^+/m^2 s, $\Phi_O/\Phi_H \sim 0.3$) [4], and (b) O^+–$H^+ \rightarrow$ C/B (CKC-B20) with beam ranges separated ($E_O = 5$ keV, $E_H = 3$ keV, $\Phi_O \sim 3 \times 10^{18}$ O^+/m^2 s, $\Phi_H \sim 3 \times 10^{19}$ H^+/m^2 s, $\Phi_O/\Phi_H \sim 0.1$). Time 'zero' corresponds to the turn-on of the O^+ beam (not shown in this figure).

To illustrate the effect of B on methane formation, CH_4 yields from both the O^+–$H^+ \rightarrow$ C and O^+–H^+ C/B cases are plotted in Fig. 3 as a function of the beam flux ratio Φ_O/Φ_H for two ion range separation cases: (a) beam ranges are completely overlapping ($R_H/R_O \sim 1$), and (b) beam ranges are completely separated ($R_H/R_O \sim 6$). In the separated case, the O^+ implant is nearer to the front surface; see Fig. 1. Note that as suggested in [4], CH_4 molecules are broken up by the

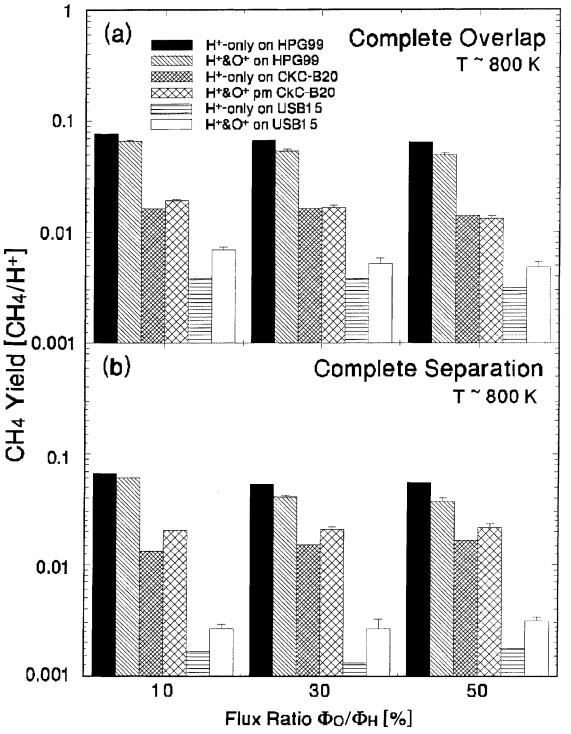

Fig. 3. CH_4 yields of both O^+–$H^+ \rightarrow$ C and O^+–$H^+ \rightarrow$ C/B irradiations as a function of beam flux ratio Φ_O/Φ_H for two ion range separation cases: (a) beams are completely overlapping ($E_O = 5$ keV, $E_H = 0.7$ keV, $R_H/R_O = 1.2$), and (b) beams are completely separated ($E_O = 5$ keV, $E_H = 3$ keV, $R_H/R_O \sim 6$). The oxygen flux Φ_O is fixed at $\sim 3 \times 10^{18}$ O^+/m^2 s, while the hydrogen flux Φ_H varies from 0.6–3.1 $\times 10^{19}$ H^+/m^2 s. Results for both CKC-B20 and USB15 are plotted for O^+–$H^+ \rightarrow$ C/B. Error bars indicate the relative error of the yield differences between the single- and dual-beam cases. The absolute error of the measurement, ~20%, is not included in the error bars.

incident O^+ ions, which causes the CH_4 yield reduction during simultaneous O^+ and H^+ irradiation in the O^+–$H^+ \rightarrow$ C case. Since this is a purely physical effect (depending entirely on the energy and cross-section of the collisions between O^+ and CH_4 molecules), this 'methane break-up' effect must still be present in the O^+–$H^+ \rightarrow$ C/B case. For the beam-overlapping case for the CKC-B20 specimen in Fig. 3(a), CH_4 yields show an *increase* during simultaneous O^+ and H^+ irradiation, but the increase just barely offsets the CH_4 yield decrease due to O^+-induced methane break-up. By comparison, for both the overlapping and separated cases of USB-15 and the separated case of CKC-B20, the methane break-up effect is more than compensated for by whatever is causing the yield increase. We note the general trend of higher methane increase for the beam-separated case. This can be explained by noting that higher methane reduction in the O^+–$H^+ \rightarrow$ C system is expected for the beam-overlapping case due to the interference of O^+ to the formation of methane precursors, in addition to the O^+-induced methane break-up [24]. Thus, the resulting CH_4 increase in the O^+–$H^+ \rightarrow$ C/B system is expected to be relatively less for the beam-overlapping case, consistent with the observed results.

Let us now examine the underlying mechanism that produces the marked difference between the O^+–$H^+ \rightarrow$ C and O^+–$H^+ \rightarrow$ C/B irradiation cases. First, let us consider the $H^+ \rightarrow$ C/B case. We propose the hypothesis that the mobile hydrogen can be trapped at internal surfaces, where an abstraction reaction with another mobile hydrogen atom may form H_2 and release it into the internal channel [2]. The production of H_2 would then depend on the population of these trapping sites and the chemistry of the carbon bonds at these sites. The presence of boron on the internal surfaces may increase the number of traps for mobile hydrogen and may also change the chemistry of the bonds at these trapping sites, which could lead to an enhancement of hydrogen recombination and ultimately to the reduction of the CH_4 yield.

With this in mind, it is interesting to observe that the presence of oxygen ions in the O^+–$H^+ \rightarrow$ C/B case seems to reduce the CH_4 yield suppression effect of boron, causing the CH_4 yield to *increase* during simultaneous O^+ and H^+ irradiation, compared to H^+-only impact. This increase is large enough that, in some cases, it more than compensates for the methane break-up effect due to energetic O^+ impact. The CH_3 precursor reduction theory of boron-induced methane yield reduction [2] does not clearly lead to this effect. Oxygen does not travel beyond the implantation range [4], and methane is produced at the end of the H^+ ion range [2,18]. Therefore, O^+ should not be able to affect the production of CH_3 precursors in the deeper hydrogen range. All these observations point to the behaviour of the mobile hydrogen on the internal surfaces as the primary cause for the CH_4 yield suppression in boron-doped graphite.

How does the incident oxygen affect the hydrogen recombination at the end of the H^+ ion range? If we assume that the modification of the internal surfaces, by the presence of boron, enhances the hydrogen recombination by creating more inner surface recombination sites (this leads to the reduction of methane yield in boron-doped graphite under H^+-only irradiation), then it is reasonable to postulate that the presence of oxygen combining with boron on the inner surfaces might 'fill' these sites, thus nullifying the enhancement of hydrogen recombination.

The reduced hydrogen recombination, due to the combined presence of B and O, would lead to an increase of the mobile hydrogen supply – distributed uniformly [18] – throughout the H^+/O^+ implantation zone. The increase of the observed methane yield for O^+–$H^+ \rightarrow$ C/B irradiation might thus be coupled to the

mobile hydrogen supply, with the implication that the mobile hydrogen partakes in the formation of CH_4. The inclusion of mobile hydrogen in the methane molecule formation, however, is consistent with the previous results obtained for H^+–D^+ co-bombardment of pure graphite where small amounts of mixed-isotope methane were detected for depthwise separated H^+–D^+ implants and seem to increase by as much as a factor of 4 until saturation is reached [19,20].

4. Summary

We have investigated the synergistic interaction occurring during simultaneous H^+ and O^+ irradiation of boron-doped graphite. Similar to our previous studies of pure graphite, we have investigated the effect of varying the ion *range ratio* and *flux ratio* of the two impacting ion species. The results indicate that the addition of O^+ to the $H^+ \rightarrow C/B$ irradiation case increases the CH_4 yield, opposite to what we found for pure graphite. The suppression of the CH_4 yield due to the presence of boron in the H^+-only irradiation case is reduced by the addition of O^+. The resulting CH_4 yield increase more than compensates for the CH_4 yield reduction due to the O^+-induced methane break-up effect. We postulate that the combined presence of oxygen and boron on the inner surfaces of graphite leads to a reduction of hydrogen recombination, and in turn, to an increase in CH_4 production.

Acknowledgements

This work was supported by ITER Canada and the Natural Sciences and Engineering Research Council of Canada. We thank Dr W. Eckstein, IPP-Garching, for making the TRVMC code available for range calculations. We also wish to thank Charles Perez for his help with the preparation of the apparatus.

References

[1] W. Eckstein, V. Philipps, in: W.O. Hofer, J. Roth (Eds.), Physical Processes of the Interaction of Fusion Plasma with Solids, Academic Press, Amsterdam, 1996, p. 93.
[2] E. Vietzke, A.A. Haasz, in: W.O. Hofer, J. Roth, Physical Processes of the Interaction of Fusion Plasmas with Solids, Academic Press, Amsterdam, 1996, p. 135.
[3] A.A. Haasz, A.Y.K. Chen, J.W. Davis, E. Vietzke, J. Nucl. Mater. 248 (1997) 19.
[4] A.Y.K. Chen, J.W. Davis, A.A. Haasz, J. Nucl. Mater. 266–269 (1999) 399.
[5] S. Chiu, A.A. Haasz, P. Franzen, J. Nucl. Mater. 218 (1995) 319.
[6] A.A. Haasz, S. Chiu, P. Franzen, J. Nucl. Mater. 220–222 (1995) 815.
[7] A.Y.K. Chen, A.A. Haasz, J.W. Davis, J. Nucl. Mater. 227 (1995) 66.
[8] J. Roth, J. Nucl. Mater. 145–147 (1987) 87.
[9] Y. Hirooka, R. Conn, R. Causey, D. Croessmann, R. Doerner, D. Holland, M. Khandagle, T. Matsuda, G. Smolik, T. Sogabe, J. Whitley, K. Wilson, J. Nucl. Mater. 176&177 (1990) 473.
[10] J.W. Davis, A.A. Haasz, J. Nucl. Mater. 175 (1990) 117.
[11] C. García-Rosales, E. Gauthier, J. Roth, R. Schwörer, W. Eckstein, J. Nucl. Mater. 189 (1992) 1.
[12] A.A. Haasz, J.A. Stephens, E. Vietzke, W. Eckstein, J.W. Davis, Y. Hirooka, in: Atomic and Plasma-Material Interaction Data For Fusion, vol. 7A, 1998.
[13] J. Roth, J. Nucl. Mater. 266–269 (1999) 51.
[14] A.A. Haasz, J.W. Davis, Nucl. Instrum. Meth. B 83 (1993) 117.
[15] A.A. Haasz, J.W. Davis, O. Auciello, P.C. Stangeby, E. Vietzke, K. Flaskamp, V. Philipps, J. Nucl. Mater. 145–147 (1987) 412.
[16] W. Eckstein, in: TRVMC: Vectorized TRIM Code for Sputtering, Multi-Component, IPP Garching, Germany, 1993.
[17] A.Y.K. Chen, A.A. Haasz, J.W. Davis, Water formation in graphite and boron-doped graphite under simultaneous O^+ and H^+ irradiation, to be published.
[18] A.A. Haasz, P. Franzen, J.W. Davis, S. Chiu, C.S. Pitcher, J. Appl. Phys. 77 (1) (1995) 66.
[19] S. Chiu, A.A. Haasz, J. Nucl. Mater. 208 (1994) 282.
[20] S. Chiu, A.A. Haasz, J. Nucl. Mater 210 (1994) 34.
[21] P. Wienhold, M. Rubel, J. von Seggern, H. Kunzli, I. Gudowska, H.G. Esser, J. Nucl. Mater. 196–198 (1992) 647.
[22] A. Refke, PhD Thesis, Forschungszentrum Julich, University of Dusseldorf, 1994.
[23] E. Vietzke, A. Refke, V. Philipps, M. Hennes, J. Nucl. Mater. 220–222 (1995) 249.
[24] A.Y.K. Chen, PhD Thesis, University of Toronto (2000).